arXiv:1401.7515v2 [cond-mat.mes-hall] 30 Jan 2014

Magneto-Photoluminescence of InAs/InGaAs/InAlAs quantum well structures

Ya. V. Terent'ev[1,2], S. N. Danilov[1], J. Loher[1], D. Schuh[1], D. Bougeard[1], D. Weiss[1], M. V. Durnev[2], S. A. Tarasenko[2], M. S. Mukhin[2], S. V. Ivanov[2], and S. D. Ganichev[1]
[1] *Physics Department, University of Regensburg, 93040 Regensburg, Germany and*
[2] *Ioffe Physical-Technical Institute, 194021 St. Petersburg, Russia*

Photoluminescence (PL) and highly circularly-polarized magneto-PL (up to 50% at 6 T) from two-step bandgap InAs/InGaAs/InAlAs quantum wells (QWs) are studied. Bright PL is observed up to room temperature, indicating a high quantum efficiency of the radiative recombination in these QW. The sign of the circular polarization indicates that it stems from the spin polarization of heavy holes caused by the Zeeman effect. Although in magnetic field the PL line are strongly circularly polarized, no energy shift between the counter-polarized PL lines was observed. The results suggest that the electron and the hole g-factor to be of the same sign and close magnitudes.

Narrow bandgap InAs-based heterostructures, being characterized by a high carrier mobility and a strong spin-orbit interaction, are generally addressed as promising systems for high-frequency electronics, optoelectronics and spintronics. In particular, QWs based on a InAs/InGaAs/InAlAs two-step bandgap engineering offer optimized confinement properties. Such QWs have been used to demonstrate a broad tunability of the emission energy in the mid-infrared range [1], high quality two-dimensional carrier systems [2–5], pronounced spin phenomena [6–9], and an electrical tunability of the electron g-factor [10]. A precise knowledge of the carrier g-factors will be a key to evaluate the application potential of such systems in spintronics. Currently, reported values of electron g-factors determined in InAs/InGaAs/InAlAs QW by magneto-transport and terahertz experiments vary in a broad range from -3.1 to -9 depending on the In-content of the QW [4, 6, 10], while g-factors deduced from magneto-optical spectroscopy are found to be much smaller in magnitude [11]. In this letter, we address the discrepancy in observed g-factors by reporting on polarization-resolved magneto-PL of samples with a high In content, for which high electron g-factors have been reported [6]. We indeed observe a strong PL polarization in a magnetic field, indicating large carrier g-factors and leading to a degree of circular PL polarization of up to 50% at 6 T. We demonstrate that the spin polarization of the heavy holes determines the observed PL polarization. Interestingly, although the carrier g-factors are found to be high, we do not observe any energy shift between the counter-polarized PL lines, resulting in a vanishing effective electron-hole g-factor. From this observation, we conclude the electron and the hole g-factor to be of the same sign and magnitude. These findings are conserved when varying the InAs QW width.

The active region was grown by molecular beam epitaxy onto a fully relaxed $In_xAl_{1-x}As$/(001)GaAs graded buffer [12] with a stepwise increase of the In content (x = 0.05 to x = 0.75) over 1 μm and consisted of a single QW as sketched in the inset of Fig. 1. The QW potential barriers are built from $In_{0.75}Al_{0.25}As$. To optimize the carrier confinement within the QW, the core of the QW, a pure InAs layer is asymmetrically embedded into a 16 nm thick $In_{0.75}Ga_{0.25}As$. To further tailor the bandstructure and hence the g-factor, different widths of the InAs layer of L_w = 3, 4 and 6 nm were used. An additional structure was modulation doped with Si below the QW at a distance of 7.5 nm from the border of the QW. The doping induces a two-dimensional electron gas (2DEG) in the QW region. An electron density of $1 \cdot 10^{12}$ cm^{-2} and a mobility of $7 \cdot 10^4$ cm^2/(V·s) at T = 14 K was determined in magneto-transport experiments. To demonstrate the resolution of our magneto PL set-up an additional $In_xAl_{1-x}As$ QW structure with Mn delta-layer in the barrier has been prepared [7, 9].

PL detected with a Fourier Transform Infrared (FTIR) spectrometer was excited by a laser diode operating in the *cw* mode at wavelength λ = 809 nm. The laser beam was focused to a 1-mm diameter spot on the sample. The excitation density W_{exc} was varied from 0.5 to 20 W/cm^2. An external magnetic field up to 6 T was applied perpendicularly to the wafer along the detected emission (Faraday geometry). The sample temperature was varied from 2 to 300 K. Right- and left-handed circular polarized emission spectra were recorded applying a quarter wave ZnSe Fresnel rhomb [13].

Bright room-temperature PL is observed from all the

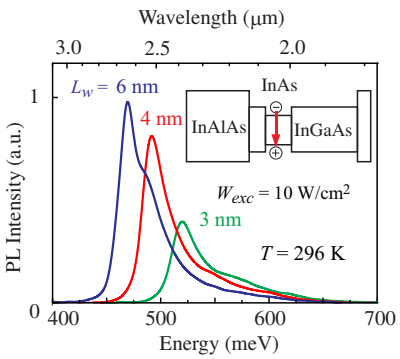

FIG. 1: PL spectra of undoped InAs QW samples. The inset shows the band diagram of the active region.

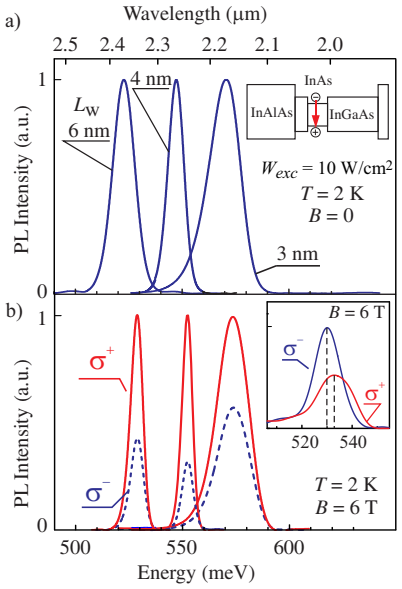

FIG. 2: (a) PL spectra of undoped InAs QWs. (b) Circularly polarized magneto-PL spectra of the same QWs. Inset shows the PL spectra from a reference structure doped with Mn.

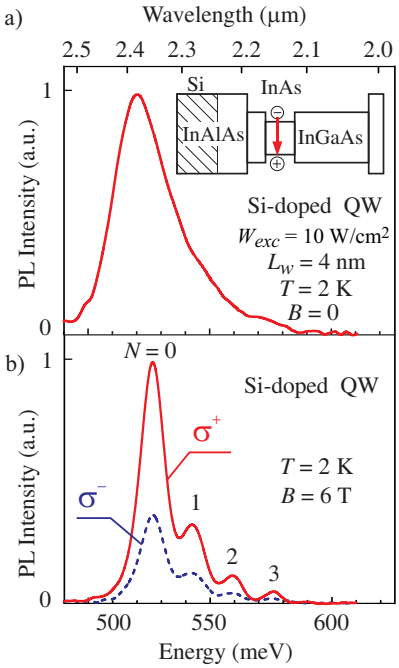

FIG. 3: (a) PL spectra of Si-doped InAs QW. (b) Circularly polarized magneto-PL spectra. The numbers N denote the transitions with the corresponding Landau level numbers.

undoped samples, see Fig. 1. Depending on the QW width, the PL spectral position varies from $\lambda = 2.4$ to 2.65 μm. According to calculations, this corresponds to direct optical transitions between the ground electron $e1$ and the heavy hole $hh1$ subbands. The PL spectral width is about 30 meV, being close to the thermal carrier energy at room temperature. By cooling the samples down to 2 K, the PL intensity increases by a factor of 20 and the linewidth decreases to 20 meV. In the whole range of excitation densities used, the PL intensity linearly depends on the excitation power, indicating a high quantum efficiency of radiative recombination in the QW structures.

The application of a magnetic field B leads to a circular polarization of the PL, as shown in Fig 2b for undoped samples, with a predominant emission of σ^+ photons along the field direction. The degree of circular polarization $P_{circ} = (I_+ - I_-)/(I_+ + I_-)$, where $I_{+/-}$ is the intensity of the $\sigma^{+/-}$ circularly polarized emission, is constant within the emission spectrum and exceeds 50% at $T = 2$ K and $B = 6$ T. Surprisingly, despite the strong circular polarization and the narrow emission lines, no energy splitting of the circularly polarized components is observed for all samples studied. Note, that a splitting down to 0.3 meV could be safely detected in our setup as it was observed, e.g., in a weakly Mn-doped reference samples of similar design, see inset in Fig. 2b.

PL is also detected from the heavily n-doped QW structure containing a 2DEG, Fig. 3a. Its intensity is about one order of magnitude weaker than the one observed from the undoped samples. Furthermore, at zero magnetic field, the PL spectrum is substantially wider and has an asymmetric shape. The linewidth corresponds approximately to the electron Fermi energy $E_F = 60$ meV. The latter value is obtained from the measured 2DEG density, 1×10^{12} cm^{-2}, and the effective electron mass $m_e^* = 0.038 m_0$, determined by magnetotransport measurements in similar structures [2, 4, 6]. The application of an external magnetic field leads to a multi-peak structure of the emission spectrum, which is caused by the formation of Landau levels, see Fig. 3b. The data reveal that the degree of PL circular polarization is almost the same for optical transitions corresponding to the Landau level number $N = 0, 1, 2$ and no energy shifts between the counter-polarized PL lines are detected. The PL polarization degree reaches 50 % at low temperatures and $B = 6$ T and is completely determined by the hole spin polarization since the electron spin levels below the Fermi energy are equally occupied. The energy distance between adjacent peaks is given by $e\hbar B/\mu$, where $\mu = m_e^* m_{hh}^*/(m_e^* + m_{hh}^*)$ is the reduced mass, and m_{hh}^* is the in-plane mass in the heavy-hole subband. From the data of Fig. 3 we find $\mu \approx 0.039 m_0$ which is close to the effective electron mass [2, 4, 6].

The observation that σ^+-polarized emission dominates in both undoped and heavily n-doped samples indicates that the PL polarization results from the spin polarization of holes in the magnetic field. This is particularly clear for the doped sample where both electron spin levels below the Fermi energy are equally occupied. It is also true for the undoped samples because the electron g-factor is known to be negative in InAs layers ($g_e \approx -15$ in bulk InAs [14] and $g_e \approx -7$ as we es-

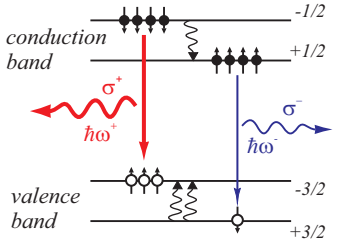

FIG. 4: Energy bands in magnetic field and allowed optical transitions. The vertical arrows indicate optical transitions with the emission of σ^+- and σ^--polarized photons. Vertical waved arrows sketch the spin relaxation process. Electron and hole population are shown schematically by circles.

timate for $In_{0.75}Ga_{0.25}As$). Indeed, in the case of PL polarization dominated by the electron spin polarization, the PL helicity would have to be opposite to the observed one. The dominating σ^+ circular polarization of the PL also indicates that the heavy hole g-factor is negative and that $|hh1, -3/2\rangle$ is the ground spin subband, as shown in Fig. 4 and expected from theory [15, 16]. The preferential population of the ground spin subband sketched in Fig. 4 is due to the fast spin relaxation of photoexcited holes. To explain the absence of a shift between the counter-polarized PL lines, we suggest that the Zeeman splittings of the electron and hole states are similar. In this case, the energies of the allowed optical transitions [17] $|e1, +1/2\rangle \rightarrow |hh1, +3/2\rangle$ and $|e1, -1/2\rangle \rightarrow |hh1, -3/2\rangle$ corresponding to σ^-- and σ^+-polarized photons, respectively, are approximately the same. To explain the absence of a shift between the counter-polarized PL lines, we suggest that the Zeeman splittings of the electron and hole states are similar. In this case, the energies of the allowed optical transitions $|e1, +1/2\rangle \rightarrow |hh1, +3/2\rangle$ and $|e1, -1/2\rangle \rightarrow |hh1, -3/2\rangle$ corresponding to σ^-- and σ^+-polarized photons, respectively, are approximately the same.

Figure 5 shows the magnetic field dependence of P_{circ} obtained for one of the undoped samples. The polarization increases linearly at low fields, $B \leq 2$ T and tends to saturate at higher magnetic fields. With decreasing temperature, the polarization considerably grows, reaching 50% at $B = 6$ T at $T = 2$ K. This behavior is in line with the microscopic model proposed above: P_{circ} is proportional to the spin polarization of holes, which is determined by $g_{hh}\mu_B B/(k_B T)$ at low magnetic fields. g_{hh} is the hole g-factor and μ_B the Bohr magneton. At higher fields, the polarization tends to saturate. The degree of the electron and hole spin-polarization depends on the respective spin relaxation, which leads to different population of the spin split subbands, and recombination processes. We note that at low temperatures, $T < 15$ K, the PL spectra recorded for both circular polarizations are weakly sensitive to the temperature, especially at low magnetic fields, see Fig. 5. This indicates that the carriers are efficiently heated by radiation.

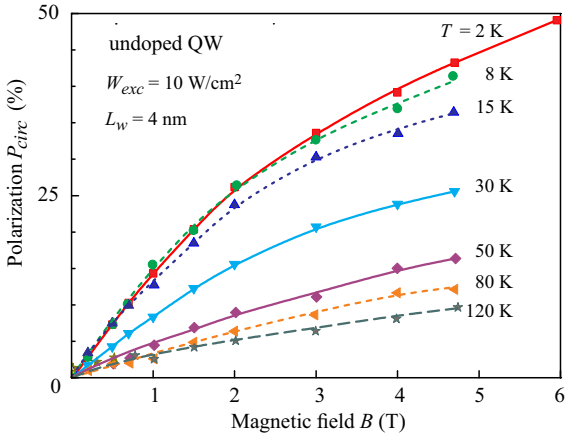

FIG. 5: Magnetic field dependencies of PL polarization measured in undoped QW. Lines are the guide for eyes.

To summarize, the observed bright PL in 2.5 μm spectral range from InAs QW structures shows that these structures are of particular importance for optoelectronics application in the mid-infrared range. Strong circular polarization of the magneto-PL together with the absence of the line spectal splitting reveal that the g-factors of electrons and heavy holes while being large have the same sign and are close to each other in magnitude.

We acknowledge financial support from the DFG (SFB 689), BMBF, RFBR, RF President Grant MD-3098.2014.2, and "Dynasty" Foundation.

[1] E. Tournié, O. Brandt, and K. Ploog, Appl. Phys. Lett. **60**, 2877 (1992).
[2] A. Richter, M. Koch, T. Matsuyama, Ch. Heyn, and U. Merkt, Appl. Phys. Lett. **77**, 3227 (2000).
[3] Ch. Heyn, S. Mendach, S. Löhr, S. Beyer, S. Schnüll, and W. Hansen, J. Crist. Growth **251**, 832 (2003).
[4] C. H. Möller, Ch. Heyn, and D. Grundler, Appl. Phys. Lett. **83**, 2181 (2003).
[5] M. Hirmer, D. Schuh, and W. Wegscheider, Appl. Phys. Lett. **98**, 082103 (2011).
[6] C.-M. Hu, C. Zehnder, Ch. Heyn, and D. Heitmann, Phys. Rev. B **67**, 201302(R) (2003).
[7] U. Wurstbauer, M. Soda, R. Jakiela, D. Schuh, D. Weiss, J. Zweck, W. Wegscheider, J. of Cryst. Growth 311, 2160(2009).
[8] U. Wurstbauer, S. Sliwa, D. Weiss, T. Dietle, and W. Wegscheider, Nature Physics **6**, 955 (2010).
[9] P. Olbrich, C. Zoth, P. Lutz, C. Drexler, V. V. Bel'kov, Ya. V. Terent'ev, S. A. Tarasenko, A. N. Semenov, S. V. Ivanov, D. R. Yakovlev, T. Wojtowicz, U. Wurstbauer, D. Schuh, and S. D. Ganichev, Phys. Rev. B **85**, 085310 (2012).
[10] J. Nitta, Y. Lin, T. Akazaki, and T. Koga, Appl. Phys. Lett. **83**, 4565 (2003).
[11] K. Tsumura, S. Nomura, T. Akazaki, and J. Nitta, Phys.

E **34**, 315 (2006).
[12] F. Capotondi, G. Biasiol, D. Ercolani, V. Grillo, E. Carlino, F. Romanato, and L. Sorba, Thin Solid Films **484**, 400 (2005).
[13] S.D. Ganichev and W. Prettl, *Intense Terahertz Excitation of Semiconductors* (Oxford Univ. Press, 2006)
[14] J. Konopka, Phys. Lett. A **26**, 21 (1967).
[15] R. Winkler, *Spin-Orbit Coupling Effects in Two-Dimensional Electron and Hole Systems*, (Springer 2003).
[16] M. V. Durnev, Phys. Solid State **56**, (2014).
[17] *Optical Orientation*, edited by F. Meier and B. P. Zakharchenya (Esevier Science, Amsterdam, 1984).